Dielectric Modulated Nanotube Tunnel Field-Effect Transistor as a Label Free Biosensor: Proposal and Investigation

Dipanjan Sen, *Student Member, IEEE,* Sharang Dhar Patel, and Shubham Sahay, *Member, IEEE*

***Abstract*— Dielectric modulated (DM) field-effect transistors (FET) have gained significant popularity for label-free detection of biomolecules. However, the inherent short channel effects limit their sensitivity, scalability and energy-efficiency. Therefore, to realize the true potential of the DMFET based biosensors, in this work, we propose a highly scalable, extremely sensitive and energy-efficient DM nanotube tunnel FET (NT-TFET) biosensor for label-free detection of biomolecules by modifying the structure of the conventional NT-TFET. The modified architecture facilitates the realization of a nanocavity at the source-channel tunneling junction and also provides stability to the immobilized biomolecules. We have performed an extensive analysis of the performance of the proposed DM NT-TFET biosensor in the presence of different representative target biomolecules characterized by different dielectric constants, and/or ionized charge densities using calibrated TCAD simulations. Our results indicate that the proposed DM NT-TFET exhibits an extremely high threshold voltage sensitivity ($S_{V_{th}}$) of 0.44, a high selectivity exceeding four orders of magnitude, ON-state current sensitivity ($S_{I_{ON}}$) of more than five orders of magnitude and could be a promising alternative to the conventional FET based dielectric modulated biosensors. Moreover, the sensitivity of the proposed DM NT-TFET could be further improved by utilizing alternate source materials with lower bandgap or by probing the transient response of the drain current and exploiting the difference in the settling time for different biomolecules with different dielectric constant (κ).**

***Index Terms*— Nanotube, Tunnel FET, Dielectric modulated, Sensitivity, Biosensor, Static power dissipation, Steric Hindrance.**

I. INTRODUCTION

Field-effect transistor (FET) based biosensors are promising solution for label-free detection of charged biomolecules owing to their low cost, high scalability, robustness, reduced response time, higher sensitivity, and high reliability [1]-[4]. Moreover, FETs with nanocavity embedded in the gate region have enabled detection of charge-free biomolecules owing to the dielectric modulation of the FET characteristics in the presence of bio-analytes. Although metal-oxide-semiconductor (MOS) FET based dielectric modulated (DM) biosensors provide pivotal information about bio-analytes, the short channel effects significantly degrade their sensitivity and limit their scalability and energy-efficiency [5]-[6].

Therefore, FETs based on alternate conduction mechanism such as tunneling, popularly known as tunnel field-effect transistors (TFETs), with diminished short-channel effects were also explored for incessantly scaling the DM biosensors [7]. DM TFET biosensors exhibit a significantly improved sensitivity owing to their steep sub-threshold slope and a low static power dissipation due to the considerably reduced OFF-state current. Moreover, the sensitivity of the DM TFET biosensors [8] could be further enhanced by utilizing a SiGe source with complementary doped pockets [9]-[10], buried strained SiGe source [11], doped Si/SiGe pockets [12]-[13], hetero-gate dielectric [14] and the multi-gate architectures such as nanowires that offer a higher tunneling efficiency and a reduced sub-threshold swing [15]-[16]. Recently, it was demonstrated that the inclusion of a core gate in addition to the outer shell gate in a vertical nanowire TFET configuration, also known as the nanotube TFET (NT-TFET) [17], significantly improves the electrostatic integrity, increases the effective tunneling area and leads to a drastic reduction in the sub-threshold swing [17]-[27]. Moreover, the architecture of NT-TFETs is essentially vertical leading to an inherent scaling benefit [24]. Considering the high scalability and significantly reduced static power dissipation in the NT-TFETs [17]-[27], it becomes imperative to explore their potential for label-free detection of bio-analytes. Therefore, several electrostatically doped nanotube TFET-based biosensors were proposed recently [25]-[26], [28]-[30]. While a junctionless nanotube TFET with a platinum-induced charge plasma source region and a dual-metal gate comprising of silver and chromium electrode in both core and shell nanocavities were used in [28], the nanocavity was introduced between the charge plasma-inducing core-source metal and the source region to enhance the sensitivity in a junctionless nanotube TFET in [29]. Moreover, a nanotube junctionless TFET with an electrostatically doped source and drain using additional program gates with a ferroelectric gate dielectric and a core source metal was used in [30] for enhancing the sensitivity. Although the electrostatically doped junctionless nanotube TFETs reported in [25]-[26], [28]-[30] exhibit a high sensitivity, they suffer from issues inherent to the electrostatically doped junctionless TFETs such as high sensitivity to process variations, large crosstalk between charge plasma or electrostatic program gate and the control gate,

Dipanjan Sen is with Department of Engineering Science and Mechanics, The Pennsylvania State University, PA 16802, USA. (e-mail: dps5991@psu.edu). Sharang Dhar Patel and Shubham Sahay are with the Department of Electrical Engineering, Indian Institute of Technology Kanpur, Kanpur 208016, India. (e-mail: ssahay@iitk.ac.in).
(Dipanjan Sen and Sharang Dhar Patel contributed equally to this work.)

limited scalability and their structure is significantly complex from a fabrication perspective.

To mitigate these issues and realize the true potential of the nanotube architecture, in this work, we propose a simple, highly scalable, and extremely energy-efficient NT-TFET based DM biosensor (DM NT-TFET) for label-free detection of biomolecules by modifying the structure of the conventional doped NT-TFETs. Unlike the conventional doped NT-TFET, the source region is located at the top while the drain region is defined at the bottom of the proposed DM NT-TFET to facilitate the immobilization of the biomolecules in the nanocavity formed in the shell gate along the vertical direction. A comprehensive analysis of the performance of the DM NT-TFET in the presence of different representative target biomolecules with a dielectric constant (κ) between 2 to 10 and an ionized charge density in the range of -10^{12} C/cm^2 to 10^{12} C/cm^2 was performed to evaluate the potential benefits of the proposed DM NT-TFET based biosensor. Our results indicate that the proposed DM NT-TFET based biosensor exhibits an extremely high threshold voltage sensitivity ($S_{V_{th}}$=0.44) and ON-state current sensitivity ($S_{I_{ON}}$= 8 × 10^5) and a high selectivity ($\Delta S_{Keratin/Streptavidin} = 3.8 \times 10^4$) as compared to the conventional MOSFET or TFET based biosensors and a significantly low OFF-state current resulting in an ultra-low static power dissipation.

The paper is organized as follows: the device structure and a process flow for realizing the proposed DM NT-TFET is presented in section II and the simulation methodology is described in section III. The results of our detailed investigation are discussed in section IV and the conclusions are drawn in section V.

II. Device Structure

The 3D schematic and the 2D cross-sectional view of the proposed DM NT-TFET biosensor are shown in Fig. 1. Since the point tunneling mechanism in TFETs is localized at the source-channel interface, the nanocavity in the gate must be placed near the source-channel interface for effective dielectric modulation. Therefore, as can be observed from Fig. 1, the source region of the DM NT-TFET is located at the top with the nanocavity embedded near the source region while the drain region is defined at the bottom unlike the conventional NT-TFET [17] where the source and drain regions are defined at the bottom and top, respectively. Furthermore, such an arrangement also improves the stability of the biomolecules accumulated in the nanocavity. Also, for the ease of contact formation, the core gate contact has been taken at the source end and a smaller core gate thickness has been used for the core gate contact to reduce the gate-to-source overlap capacitance and improve the dynamic performance of the proposed DM NT-TFET biosensor.

The proposed DM NT-TFET may be realized using the process flow suggested in [17] and [20] with addition of two steps: (a) deposition of a sacrificial layer while defining the shell gate stack and (b) selective etching of the sacrificial layer after the contact formation. We have also suggested a process flow for realizing the proposed DM NT-TFET as shown in Fig. 2. Since similar vertical nanostructures and hollow silicon nanorods have already been demonstrated experimentally in [31] utilizing reactive ion etching and high-precision plasma-treated lithography, the experimental realization of the proposed DM NT-TFET utilizing the suggested process flow should not pose a significant fabrication complexity. As shown in Fig. 2, first, the cylindrical-silicon region may be realized using electron beam lithography (EBL) and sacrificial sidewall deposition (Figs. 2.1 – 2.3). Then, the shell gate oxide and the sacrificial layer (which is etched later to form the nanocavity) can be deposited followed by deposition of the shell gate (Figs. 2.4 - 2.6). The shell gate and the outer gate oxide can then be etched followed by deposition of another sacrificial layer (which acts like top spacer) as shown in Fig. 2.7. Subsequently,

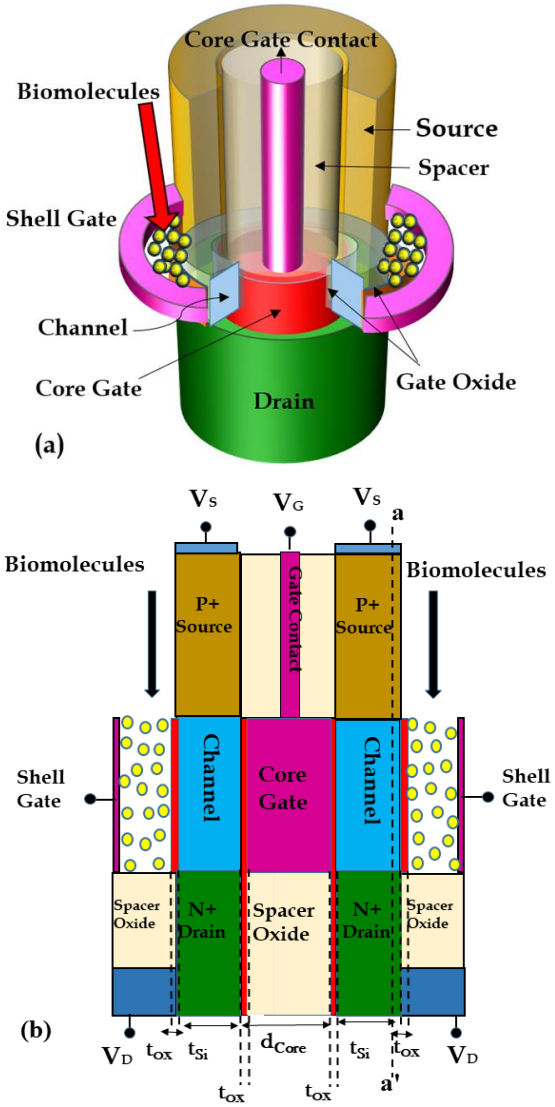

Fig. 1 (a) 3D and (b) 2D schematic view of the proposed nanotube tunnel FET (NT-TFET) based DM biosensor.

chemical mechanical polishing (CMP) may be utilized for planarization and the sacrificial layer may be etched followed by growth of an epitaxial silicon region (Fig 2.8). Later, a hard mask (TEOS) layer may be deposited and the inner portion of the epitaxially grown silicon may be etched to form a trench (Figs. 2.9 - 2.11). The core gate dielectric can then be deposited

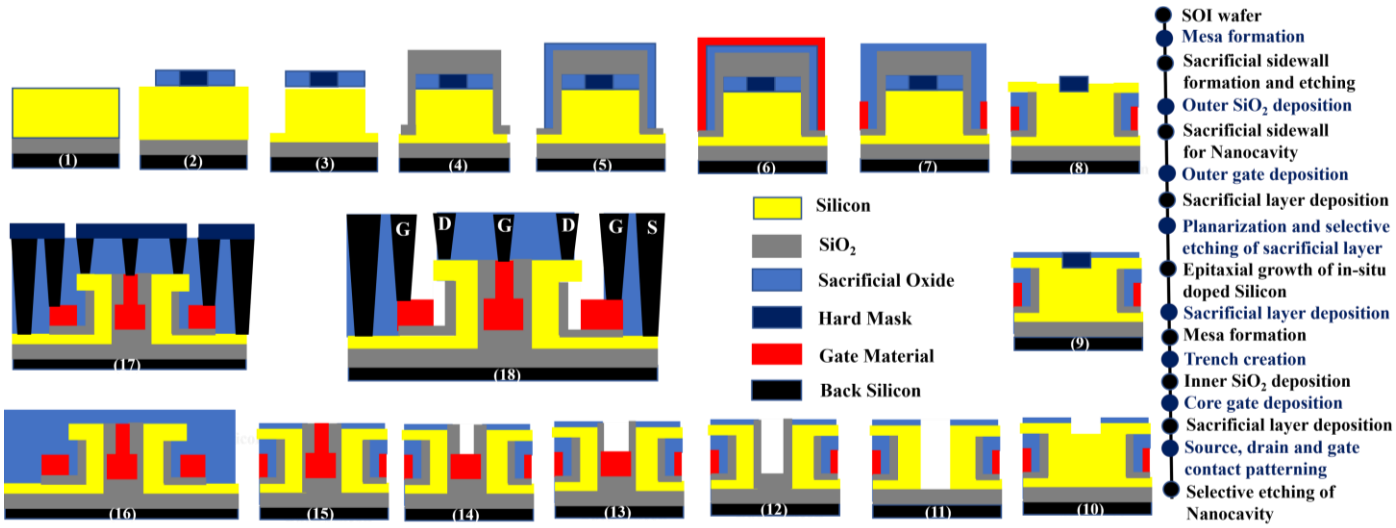

Fig. 2 A suggested process flow for realizing the proposed DM NT-TFET based biosensor following [17] and [20] by adding two process steps.

followed by the deposition of the core gate (Figs. 2.12 - 2.13). To realize a thinner core gate close to the core gate contact, oxide deposition may be followed with core gate deposition (Figs. 2.14 - 2.15). The contacts may be defined after passivation (Figs. 2.16 - 2.17). Finally, the nanocavity can be realized by etching the sacrificial layer between the source contact and shell gate contact as shown in Fig. 2.18.

To analyze the performance of the proposed DM NT-TFET, a channel length of 50 nm has been used [17]-[18]. A core gate diameter (d_{Core}) of 100 nm, a silicon film thickness (t_{Si}) of 10 nm, an effective oxide (SiO_2) thickness of 1 nm and a length of 50 nm has been considered [16]. It has been experimentally demonstrated that a small nanocavity is desirable for improving the sensitivity and enhancing the signal-to-noise ratio (SNR) of the FET-based biosensors [32]-[33]. Furthermore, since the size of the typical protein molecules such as biotin and streptavidin lie in the range of ~3 – 5 nm, a nanocavity with a thickness of 10 nm is sufficient to facilitate immobilization of biomolecules for detection using FET-based biosensors. Moreover, efficient detection of biomolecules using nanocavity thickness of 7 nm and 10 nm has already been demonstrated experimentally in [33]. Therefore, we have utilized a nanocavity with a thickness of 10 nm in this work. Also, a gate metal with a work function of 3.9 eV has been used for both core and shell gates. The

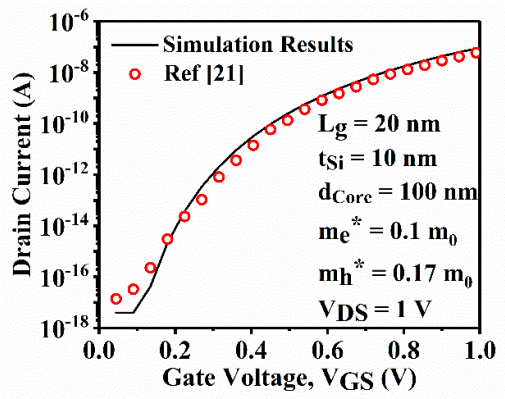

Fig. 3 Simulation setup calibrated by reproducing the results of NT-TFETs in [21].

source, channel and drain regions were uniformly doped to N_A = 5 x 10^{19} cm^{-3}, N_A = 10^{15} cm^{-3} and N_D = 5 x 10^{19} cm^{-3}, respectively.

III. Simulation Framework

The performance of the proposed DM NT-TFET was analyzed with the aid of SILVACO ATLAS TCAD tool [34]. The nonlocal band-to-band tunneling (BTBT) model based on the Wentzel-Kramers-Brillouin (WKB) approximation was used to consider the point tunneling at the source-channel interface. In addition, the doping-dependent and the field-dependent mobility degradation models were also included. The Shockley-Read-Hall (SRH) recombination and Auger recombination

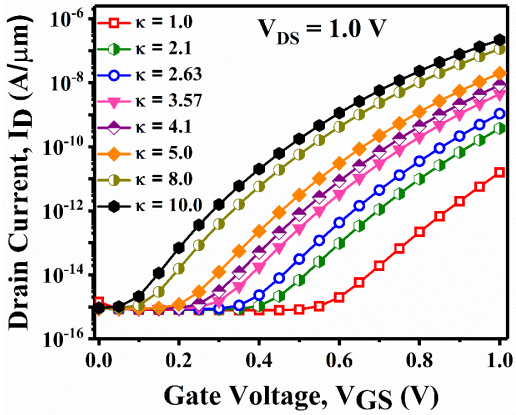

Fig. 4 Transfer characteristics of the proposed DM NT-TFET in the presence of different neutral biomolecules with different dielectric constant (κ).

models were enabled and the band-gap narrowing (BGN) model was activated to take into account the band gap reduction in the heavily doped source and drain regions. Furthermore, the physical model parameters such as effective tunneling mass of electrons and holes (0.1 m_0 for electrons and 0.17 m_0 for holes), were tuned and the simulation set up was calibrated by reproducing the characteristics of NT-TFET reported in [21] as shown in Fig. 3. Moreover, we obtained the absolute drain current (in A) by multiplying the normalized drain current with the effective silicon circumference given as $\pi(d_{core}+t_{Si})$ [22]-[24].

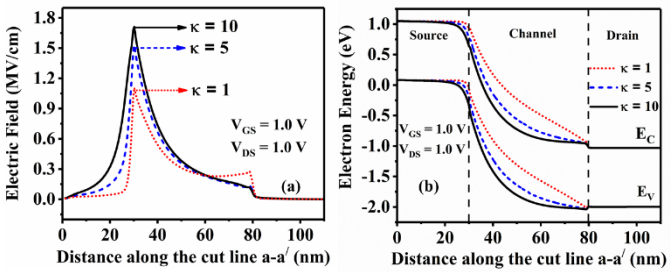

Fig. 5 (a) Electric field and (b) energy band profiles of the proposed DM NT-TFET based biosensor in the presence of neutral biomolecules with different dielectric constant (κ).

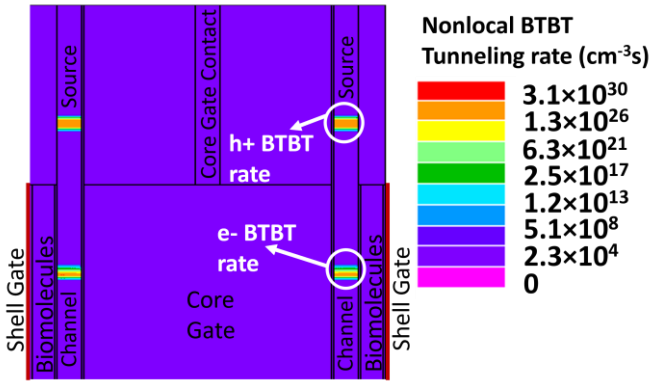

Fig. 6 BTBT generation rate profile of DM NT-TFET with keratin (κ = 10) filled nanocavity for $V_{DS} = V_{GS} = 1$ V.

The immobilization of biomolecules inside the nanocavity was modeled as a change in the dielectric constant (κ) with κ varying between 2 to 10 which includes biomolecules such as streptavidin (κ = 2.1), biotin (κ = 2.63), APTES (κ = 3.57), gluten (κ = 5), Apo myoglobin (κ = 8), keratin (κ = 10), etc. Furthermore, we have assumed (dry sensing) air environment with a dielectric constant κ = 1 to emulate the absence of biomolecules in the nanocavity following the prior works [10]-[11], [13], and [35]. In experimental measurements, such an air ambient is achieved by washing with de-ionized water several times and drying with N_2 gas [35]-[37]. It may be noted that the main objective of this work is to demonstrate the relative change in the characteristics of the DM NT-TFET in the presence of different biomolecules in the nanocavity rather than showing the exact values of the current.

IV. Results and Discussion

The transfer characteristics of the proposed DM NT-TFET in the presence of biomolecules with different dielectric constant in the nanocavity are shown in Fig. 4. As can be observed from Fig. 4, the ON-state ($V_{DS} = V_{GS} = 1$ V) current of the proposed DM NT- TFET increases monotonically with an increase in the dielectric constant (κ) of the biomolecule in the nanocavity. The ON-state current increases significantly by more than four orders of magnitude when κ changes from 1 (air-filled nanocavity) to 10 (keratin-filled nanocavity) as shown in Fig. 4. This is attributed to the enhanced gate coupling in the presence of keratin-filled nanocavity (κ = 10) which results in an increased vertical electric field at the source-channel tunneling junction as shown in Fig. 5(a). The high electric field leads to a significant reduction in the tunneling width as shown in Fig. 5(b) resulting in a considerable increase in the ON-state current by more than four orders of magnitude. Although low ON-current values such as 10^{-9} to 10^{-10} A have been considered for biosensor with air (k=1) filled nanocavity [44]-[45], the signal to noise ratio would be limited for such biosensors during practical measurements. Moreover, utilizing such biosensors for practical application would necessitate the use of a complex sense amplifier circuitry with high gain and low SNR.

The BTBT generation rate profile is shown in Fig. 6. for the proposed DM-NT TFET biosensor with keratin (κ = 10) in the nanocavity. The non-local BTBT model in ATLAS treats the quantum-mechanical BTBT phenomena as a classical generation process and displays the BTBT generation of

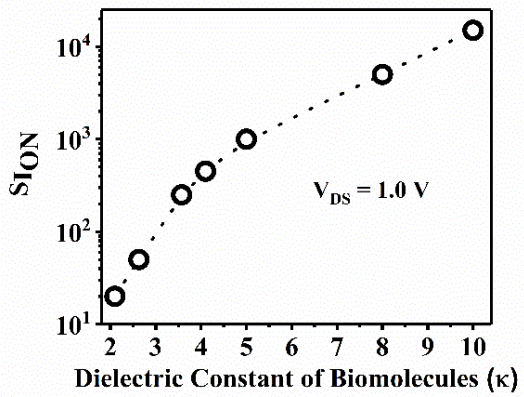

Fig. 7 ON-state current sensitivity ($S_{I_{ON}}$) of the proposed DM NT-TFET based biosensor in the presence of neutral biomolecules with different dielectric constant (κ).

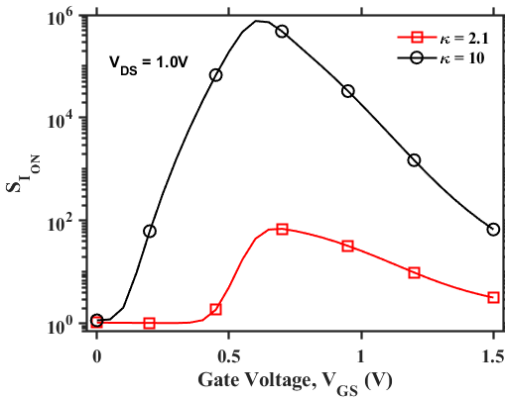

Fig. 8 ON-state current sensitivity ($S_{I_{ON}}$) of the proposed DM NT-TFET based biosensor with varying gate voltage.

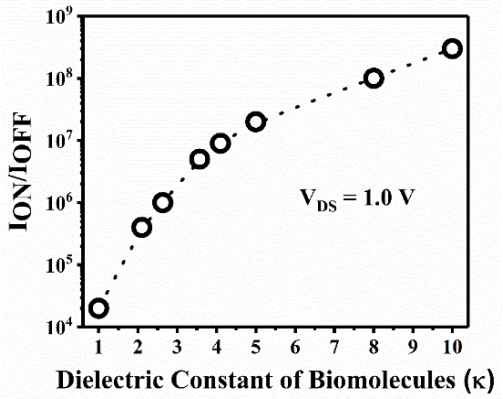

Fig. 9 ON-state current to OFF-state current ratio (I_{ON}/I_{OFF}) of the proposed DM NT-TFET in the presence of neutral biomolecules with different dielectric constant (κ).

electrons and holes at the end of the user-defined quantum tunneling mesh as can be observed from Fig. 6. The BTBT generation rate for electrons and holes is significantly high in the presence of biomolecule in the nanocavity.

A. ON-State Current Sensitivity

Furthermore, the ON-state current sensitivity ($S_{I_{ON}}$), defined as:

$$S_{I_{ON}} = \left|\frac{I_{ON}(bio)}{I_{ON}(air)}\right| \quad (1)$$

where, I_{ON} (bio) is the ON-state current in the presence of biomolecules in the nanocavity and I_{ON} (air) is the ON-state current in the absence of biomolecules in the nanocavity (air-filled nanocavity), is an important sensing metric for DM TFET-based biosensors since it is relatively immune to the variations in the operating temperature [38]. As shown in Fig. 7, $S_{I_{ON}}$ increases with an increase in the dielectric constant (κ) of the biomolecule in the nanocavity. The proposed DM NT-TFET exhibits a significantly high ON-state current sensitivity of more than four orders of magnitude ($S_{I_{ON}} = 2 \times 10^4$) when the nanocavity is filled with keratin (κ = 10). Also, as shown in Fig. 8, the ON-state current sensitivity ($S_{I_{ON}}$) depends significantly on the gate voltage selected as the ON-state voltage. Furthermore, the peak ON-state current sensitivity (~8×10^5) is obtained at a lower gate voltage (V_{GS} = 0.6 V) as compared to the supply voltage ($V_{GS} = V_{DD}$ = 1.0 V). The drain current for DM NT-TFET with air-filled nanocavity increases at a slower rate with the gate voltage for low V_{GS} (<0.6 V) while the drain current for DM NT-TFET with keratin filled nanocavity increases rapidly with the gate voltage for low V_{GS} (<0.6 V). This results in an increase in the ON-state current sensitivity of the DM NT-TFET based biosensor till V_{GS} = 0.6 V. However, at higher V_{GS} (>0.6V), the drain current for DM NT-TFET with air-filled nanocavity increases at a larger rate than the DM NT-TFET with keratin filled nanocavity as shown in Fig. 4. This leads to a reduction in the ON-state current sensitivity.

Also, the OFF-state current of the proposed DM NT-TFET is significantly low (by nearly four orders of magnitude) as compared to a MOSFET DM biosensor [39]. A lower OFF-state current leads to a significantly reduced static power dissipation in the DM NT-TFET based biosensor.

Moreover, the ON-state to OFF-state current ratio (I_{ON}/I_{OFF}) of the DM NT-TFET is considerably high and increases with an increment in κ of the biomolecules. The proposed DM NT-TFET exhibits a significantly high I_{ON}/I_{OFF} of 6×10^8 for keratin-filled nanocavity (κ = 10) as shown in Fig. 9. The ON-state to OFF-state current ratio (I_{ON}/I_{OFF}) can also be used as a sensing metric for detection of the bio-analytes. The proposed DM NT-TFET exhibits more than four orders of magnitude change in I_{ON}/I_{OFF} for keratin-filled nanocavity (κ= 10) as compared to the air-filled nanocavity (κ= 1).

B. Threshold Voltage Sensitivity

Furthermore, the threshold voltage (V_{th}), measured using the constant current method [24], of the DM NT-TFET decreases monotonically with an increase in the κ of the biomolecules

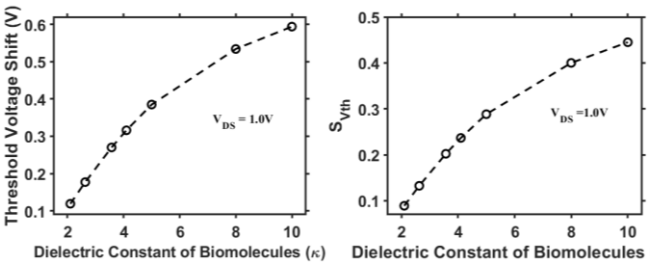

Fig. 10 (a) The threshold voltage (V_{th}) Shift and (b) threshold voltage sensitivity (S_{Vth}) of the proposed DM NT-TFET based biosensor in the presence of different neutral biomolecules with different dielectric constant (κ).

inside the nanocavity as shown in Fig. 4. The threshold voltage sensitivity (S_{Vth}) of the proposed DM NT-TFET based biosensor in the presence of different biomolecules in the nanocavity can be defined in terms of the shift in the threshold voltage as [35]:

$$S_{V_{th}} = \left|\frac{V_{th}(air) - V_{th}(bio)}{V_{th}(air)}\right| \quad (2)$$

where, $V_{th}(air)$ and $V_{th}(bio)$ are the threshold voltages of the DM NT-TFET in the absence of biomolecules in the nanocavity (air-filled nanocavity) and the presence of biomolecules in the nanocavity, respectively. $S_{V_{th}}$ represents the relative change in the threshold voltage and is a more fundamental quantity (similar to the relative error) than the absolute threshold voltage shift (or absolute error) for benchmarking [35]. However, the definition of $S_{V_{th}}$ will not be valid if the threshold voltage of the biosensor for air-filled nanocavity is zero. Since the threshold voltage is obtained using the constant current method, one can always tune the reference current value used for defining the threshold voltage (and make it non-zero for air-filled nanocavity). Moreover, the absolute threshold voltage shift (Fig. 10(a)) can be used as the benchmarking parameter when the threshold voltage of the biosensor in the presence of air-filled nanocavity is zero. As shown in Fig. 10(a), while the shift in the threshold voltage (as compared to the DM NT-TFET with air-filled nanocavity) for DM NT-TFET with keratin-filled nanocavity (κ = 10) is significantly high (594 mV), the shift in the threshold voltage for DM NT-TFET with streptavidin-filled nanocavity (κ = 2.1) is also appreciable (119 mV). Therefore, the proposed DM NT-TFET can also detect biomolecules with low dielectric constant efficiently. As can be observed from Fig. 10(b), the threshold voltage sensitivity (S_{Vth}) of the DM NT-TFET based biosensor improves with an increase in the dielectric constants of the biomolecules. The threshold voltage sensitivity is maximum ($S_{Vth} = 0.44$) for keratin-filled nanocavity (κ = 10) and minimum ($S_{Vth} = 0.1$) for streptavidin-filled nanocavity (κ = 2.1). Furthermore, the threshold voltage

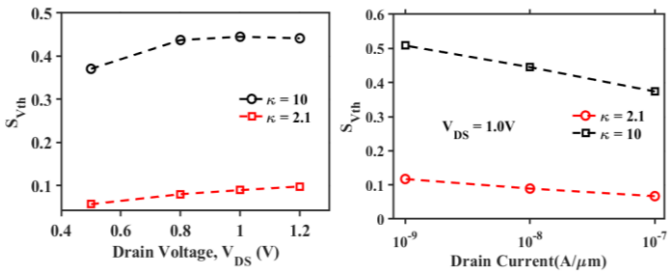

Fig. 11 Threshold voltage sensitivity (S_{Vth}) of the proposed DM NT-TFET based biosensor with varying (a) drain voltage (b) reference drain current for V_{th} measurement.

of ultra-short channel TFETs is also sensitive to the drain voltage owing to the short channel effects such as drain-induced barrier thinning (DIBT) [24], [40]. The variation of the threshold voltage sensitivity (S_{Vth}) with applied drain voltage (V_{DS}) is shown in Fig. 11(a). S_{Vth} increases with an increase in the drain voltage and saturates at high V_{DS} values. Since we have used the constant current method for measuring the threshold voltage, changing the reference drain current value for calculating the threshold voltage also changes S_{Vth} as can be observed from Fig. 11(b). Although S_{Vth} for the proposed DM NT-TFET based biosensor does not change significantly with streptavidin-filled nanocavity (κ = 2.1), S_{Vth} reduces significantly from 0.51 to 0.37 as the reference drain current for measuring the threshold voltage is changed from 10^{-9}A/μm to 10^{-7} A/μm for the proposed DM NT-TFET based biosensor with keratin-filled nanocavity (κ = 10).

C. Selectivity

Selectivity is also an important performance metric of the FET-based biosensors and represents the ability of the biosensor to distinguish between different biomolecules. Selectivity of a FET-based biosensor for biomolecule B1 over biomolecule B2 is defined as [41]:

$$\Delta S_{B1/B2} = \left|\frac{I_{ON(B1)} - I_{ON(B2)}}{I_{ON(B2)}}\right| \quad (3)$$

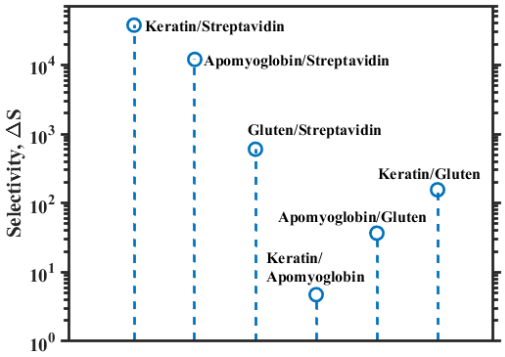

Fig. 12 Selectivity (ΔS) of the proposed DM NT-TFET based biosensor.

Fig. 12 shows the selectivity of the proposed DM NT-TFET based biosensor for different biomolecules used in this work. While the selectivity of keratin (κ = 10) over streptavidin (κ = 2.1) is maximum (3.8×10^4), the proposed biosensor exhibits the minimum selectivity between keratin (κ = 10) and Apo myoglobin (κ = 8). The selectivity of the proposed DM NT-TFET biosensor increases with an increase in the relative difference of the dielectric constants of the biomolecules under consideration [41].

D. Impact of Charge on Biomolecules

Additionally, some target biomolecules (such as DNA) get ionized when linked with specific receptor atoms and the charge on the biomolecule depends on the combination of receptor and biomolecule. Furthermore, DM MOSFET based biosensors are highly sensitive to the charges on the biomolecules and the device type (n- or p-MOSFET) needs to be changed to effectively capture the different polarity of charges depending on the ionized biomolecules [4]. These charges are generally

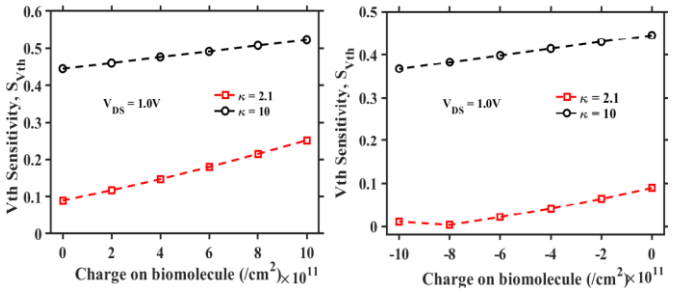

Fig. 13 Threshold voltage sensitivity (S_{Vth}) of the DM NT-TFET based biosensor in presence of ionized biomolecules with (a) positive charge and (b) negative charge.

localized at the surface of the gate dielectric (and can be modelled as line charges on the gate oxide material) and modulate the surface potential of the channel region.

Furthermore, the charge density of the biomolecule depends on their isoelectric point (pI), the pH and the molar concentration of the solution. The charge density may be altered by tuning the difference between the isoelectric point and the pH of the solution or by changing its molar concentration. A potential methodology to decouple the impact of charges and dielectric constant on the threshold voltage shift could be to reduce the charges on the biomolecule by keeping the pH of the solution close to the pI of the biomolecule. However, for efficient detection of biomolecules by using the charge-dominant threshold voltage shift, the difference between pI of the biomolecule and the pH of the solution should be kept large or a high molar concentration of solution should be used [32], [42]. Although previous studies [32], [42] have suggested methods such as charge pumping to find the polarity of charges, specific charge density on individual biomolecules due to different pH and molar concentration of the solutions has not yet been reported. Therefore, modeling a biomolecule with a particular fixed charge density is not feasible [32], [42] and a charge density range of 10^{10}-10^{12} C cm^{-2} is usually taken to analyze the impact of charges on the biomolecules on the sensitivity of FET-based biosensors [32].

Moreover, the dominant mechanism (charge or dielectric constant) which leads to shift in the threshold voltage also depends on the type of biomolecules under consideration. For instance, biomolecule-charge would be the dominant factor driving the shift in the threshold voltage while sensing bio-analytes such as DNAs. However, dielectric constant would be the dominant factor while sensing protein molecules or ligands such as APTES or Streptavidin where charge density of the biomolecule is small since their pI is close to pH (= 7) of neutral solutions [32], [42].

Therefore, we have analyzed the performance of the proposed DM NT-TFET biosensor in the presence of both charged biomolecules with different charge density and neutral biomolecules with different biomolecules to decouple their impact on threshold voltage shift. Fig. 13 illustrates the impact of ionized biomolecules on the threshold voltage sensitivity (S_{Vth}) of the DM NT-TFET based biosensor. While the positively charged biomolecules boost the surface potential leading to an enhanced tunneling current and a reduced threshold voltage, the negatively charged biomolecules result in an increased threshold voltage. Therefore, the threshold voltage sensitivity (S_{Vth}) increases with an increased density of

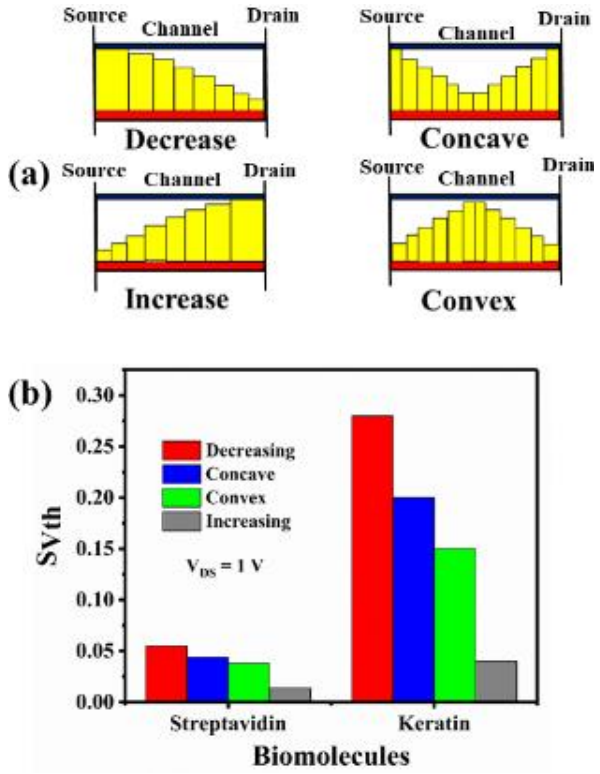

Fig. 14 (a) Different immobilized biomolecule profiles due to steric hindrance and (b) threshold voltage sensitivity of DM NT-TFET based biosensor for streptavidin (κ = 2.1) and keratin (κ = 10) in the presence of steric hindrance.

positively charged biomolecules in the nanocavity of DM NT-TFET. The proposed DM NT-TFET shows a significantly high sensitivity ($S_{Vth} = 0.44$) when the keratin-filled nanocavity (κ = 10) gets ionized to a positive charge density of 10^{12} C/cm^2. Although S_{Vth} degrades in the presence of negatively charged biomolecules inside the nanocavity, the sensitivity ($S_{Vth} = 0.37$) is still appreciably high for the proposed DM NT-TFET with keratin-filled nanocavity (κ = 10) as compared to the other conventional MOSFET/TFET based biosensors (table II).

E. Impact of Steric Hindrance

As discussed in section III, in FET-based biosensors, the target bio-analytes tend to attach with the receptor or linker molecules and get immobilized enabling the sensing mechanism. However, in the practical scenario, all the target bio-analytes are not able to attach with the appropriate receptor molecules due to steric hindrance and the variation in the physical properties of the receptor, target bio-analytes, and electrolytic solutions [43]. This partial hybridization of target bio-analytes generates an asymmetric pattern of immobilized biomolecules inside the nanocavity which affects the sensitivity of the biosensor. To consider this non-ideal behavior, we have taken four standard patterns for analyzing the sensitivity of the proposed biosensor as illustrated in Fig. 14(a).

The threshold voltage sensitivity (S_{Vth}) is lowest in the case of the immobilized bio-analytes with increasing profile and highest for the case of immobilized biomolecules with decreasing profile for both Streptavidin and Keratin as shown in Fig. 14(b). In the decreasing/concave profiles of immobilized biomolecules, a larger concentration of biomolecules is immobilized near the source/channel interface as compared to the increasing and convex profile. Therefore, a large number of electric field lines from the gate electrode penetrates the channel region at the source-channel interface in the DM NT-TFET with concave/decreasing profiles of immobilized biomolecules. Since the point tunneling mechanism is highly sensitive to the amount of band bending at the source-channel interface, the proposed DM NT-TFET exhibits a higher sensitivity to the concave and decreasing profiles of the immobilized bio-analytes.

F. Impact of Structural Parameters

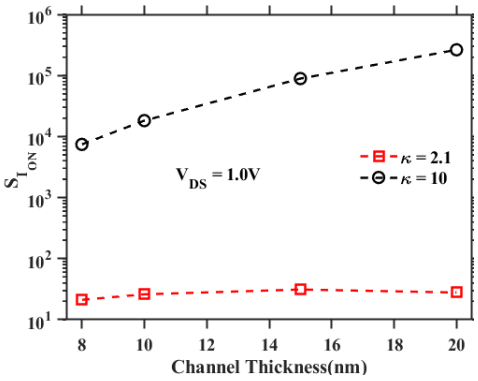

Fig. 15 ON-state current sensitivity ($S_{I_{ON}}$) of the proposed DM NT-TFET based biosensor with different channel thickness.

The ON-state current sensitivity also depends on the channel thickness. As shown in Fig. 15, the ON-state current sensitivity increases with increasing channel thickness. An increase in the channel thickness increases the curved-surface area of the source-channel junction [$2\pi(0.5\, d_{Core} + t_{ox} + t_{Si})(L_{tunn})$] at which point tunneling takes place [18]. This results in an increase in the drain current for the DM-NT TFET based biosensor. Moreover, the increase in the current is more for DM NT-TFET with streptavidin-filled nanocavity as compared to the DM NT-TFET with air-filled nanocavity. As a result, the on-state current sensitivity of the DM NT-TFET increases with the channel thickness. While $S_{I_{ON}}$ does not increase significantly for the proposed DM NT-TFET based biosensor

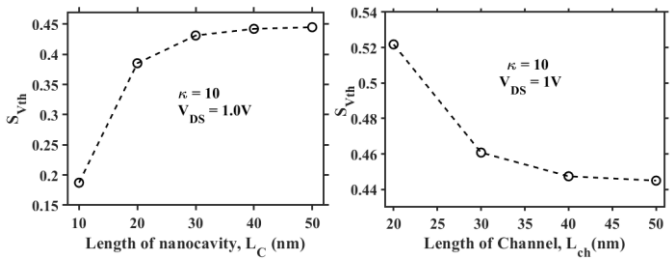

Fig. 16 Threshold voltage sensitivity (S_{Vth}) of the proposed DM NT-TFET based biosensor with different (a) nanocavity lengths, L_C (b) channel lengths, L_{ch}.

with streptavidin-filled nanocavity (κ = 2.1), it increases considerably by more than an order of magnitude when the channel thickness is increased from 8 nm to 20 nm for the DM NT-TFET based biosensor with keratin-filled nanocavity (κ = 10). The threshold voltage sensitivity also depends on the nanocavity length as shown in Fig. 16(a). As can be observed from Fig. 16(a), the sensitivity improves with an increase in the nanocavity length. Moreover, the relative change in the

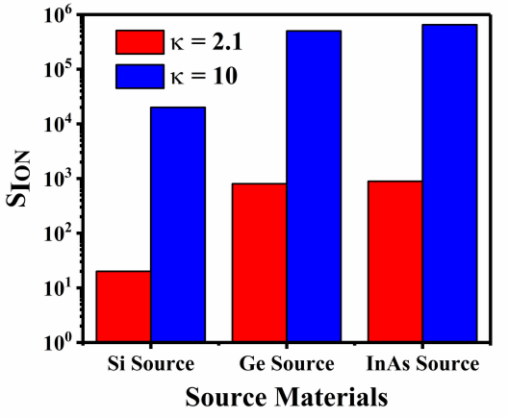

Fig. 17 ON-state current sensitivity ($S_{I_{ON}}$) with different source materials.

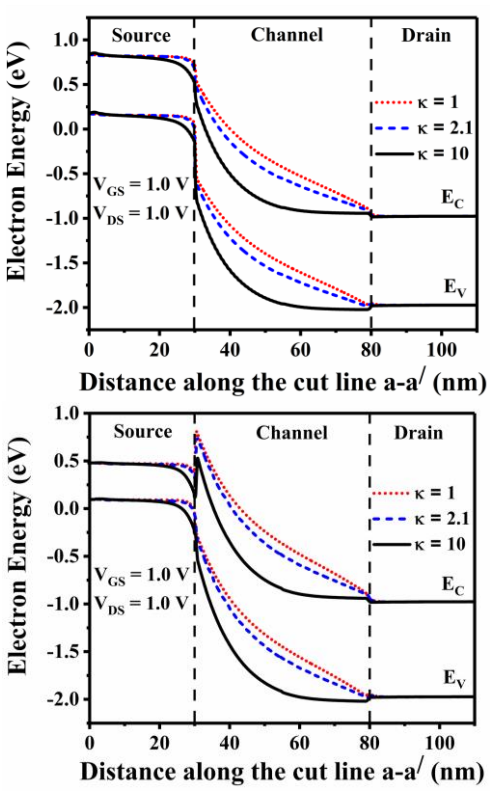

Fig. 18 Energy band profiles of the DM NT-TFET based biosensor for (a) Ge source, (b) InAs source

sensitivity is nearly 16% for keratin-filled nano-cavity (κ = 10) when the nanocavity length increases from 20 nm to 50 nm.

Although point tunneling occurs at the source-channel interface, the threshold voltage sensitivity is affected due to channel length scaling owing to the short channel effects such as drain-induced barrier thinning (DIBT) [24],[40]. DIBT leads to a significant increase in the drain influence on the electrostatics of TFETs resulting in an increased leakage current and a reduction in the threshold voltage. Since the reduction in the threshold voltage is more for κ = 1 than for κ = 10, we observe a reduction in the threshold voltage sensitivity with increasing channel length as shown in Fig. 16(b). The relative change in the sensitivity is nearly 14% for keratin-filled nano-cavity (κ = 10), when the channel length is increased from 20 nm to 50 nm. Also, it may be noted that the proposed DM NT-TFET is a vertical structure, and the footprint is not dictated by the length of nanocavity or channel. The enhanced scalability of the proposed DM NT-TFET is attributed to the significantly suppressed leakage current which is critical for large-scale logic circuits and the inherent vertical architecture where the critical dimensions such as channel length is defined by the well-controlled deposition process instead of lithography.

G) Impact of Source Material

Since the ON-state current and the sub-threshold swing of the NT-TFETs can be significantly improved by utilizing source materials with lower bandgap such as germanium (Ge) and indium arsenide (InAs) [18]-[19], we have also analyzed the performance of the proposed DM NT-TFET with different source materials as shown in Fig. 17. The effective tunnelling mass for Ge and InAs were also tuned to reproduce the results reported in [18] and [19]. The m_e and m_h values used for Ge were 0.06 m_0 and 0.2 m_0, respectively while for InAs, m_e and m_h values of 0.026 m_0 and 0.4 m_0, respectively, were utilized in this work. The ON-state current sensitivity ($S_{I_{ON}}$) increases significantly by more than five orders of magnitude when κ changes from 1 (air-filled nanocavity) to 10 (keratin-filled nanocavity) when InAs and Ge are selected as the source materials. The lower bandgap of InAs and Ge leads to a significant reduction in the tunneling width as shown in Fig. 18(a-b) resulting in a considerable increase in the ON-state current sensitivity. In addition, $S_{I_{ON}}$ increases by 2900% for Ge source and 3900% for InAs source as compared to the DM NT-TFET with silicon source.

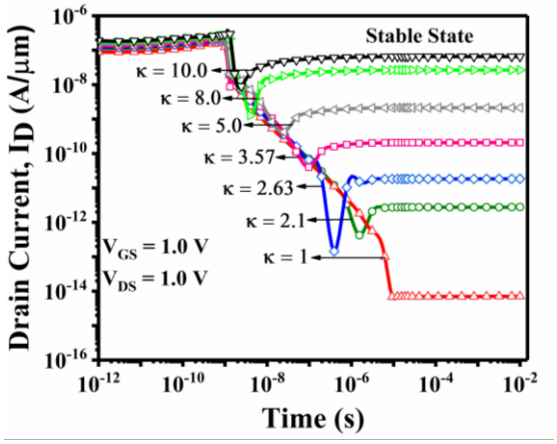

Fig. 19 Transient response of the drain current of the proposed DM NT-TFET in presence of different neutral biomolecules with different dielectric constant (κ).

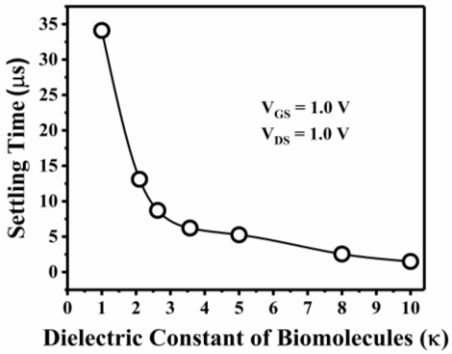

Fig. 20 Settling time of the proposed DM NT-TFET based biosensor in presence of different neutral biomolecules with different dielectric constant (κ).

H) Transient Response

Also, it was shown recently that the sensitivity and selectivity of the DM TFET based biosensors could be significantly improved by probing their transient response and exploiting the different settling times of the drain current in the presence of different biomolecules in the nanocavity [41]. Therefore, we have also analyzed the transient response of the proposed DM NT-TFET biosensor in the presence of different biomolecules in the nanocavity as shown in Fig. 19. The drain current in the stable state increases with an increase in the dielectric constant of the biomolecules. Also, the settling time of the drain current in the transient response decreases with an increase in the dielectric constant of the biomolecules as shown in Fig. 20. This is attributed to the enhanced vertical electric field and the BTBT rate of the DM NT-TFET in the presence of biomolecules with high κ. Moreover, the ON-state current sensitivity increases significantly to nearly seven orders of magnitude, when κ changes from 1 (air-filled nanocavity) to 10 (keratin-filled nanocavity) while probing the transient analysis (at a time instance of 0.1μs).

TABLE I
PERFORMANCE ANALYSIS OF PUBLISHED FET BASED BIOSENSORS CONSIDERING I_{ON} SENSITIVITY

Sl. No.	TFET Based Biosensors	ON-state current Sensitivity (S_{ION})
1	Lateral DM HTFET (L_{gap} = 20 nm, L_{Ch} = 42 nm, κ = 2.1) [10]	10
2	Single Pocket DM TFET (L_{gap} = 20 nm, L_{Ch} = 42 nm, κ = 2.1) [10]	40
3	SiGe Source DM PNPN TFET (L_{gap} = 20 nm, L_{Ch} = 42 nm, κ = 2.1) [12]	4×10^3
4	DM FET (Lgap = 30 nm, Lgate = 100 nm, κ = 10) [8]	5
5	DM FET (L_{gap} = 75 nm, L_{gate} = 250 nm, κ = 10) [8]	7
6	Double Gate (DG) TFET (L_{gap} = 30 nm, L_{gate} = 40 nm, κ = 12) [13]	1.05×10^2
7	DM NT-TFET (L_{gap} = 50nm, L_{gate} = 50nm, κ = 10) (V_{GS} = 0.6 V) (This work)	$\sim 8 \times 10^5$
8	Ge source DM NT-TFET (L_{gap} = 50nm, L_{gate} = 50nm, k = 10) (This work)	6×10^5
9	InAs source DM NT-TFET (L_{gap} = 50nm, L_{gate} = 50nm, k = 10) (This work)	8×10^5
10	Charge plasma based DM NT-TFET (L_{gap} = 10nm, 50nm, L_{gate} = 20nm & 11nm, k = 8)[28]	~50
11	Diagonal Tunneling based DM NT-TFET (L_{gap}=95nm, L_{gate} = 50nm+45nm, k = 10) [44]	$\sim 10^{10}$
12	Dual ChannelTrench Gate Biosensor (L_{gap} = 90nm, L_{gate} = ~90nm, k = 12)[45]	7×10^{12}
13	N+ Pocket Doped Vertical TFET (L_{gap} = 20nm & 30nm, L_{gate} = 40nm & 30nm, k = 10)[13]	3×10^5
14	Core-Shell Junctionless NT-TFET (L_{gap} = 100nm, L_{gate} = 50nm, k = 8,50%filled)[26]	$\sim 2 \times 10^2$

L_{gap}: length of nanocavity, L_{ch}: channel length, κ: dielectric constant of detected biomolecule

I) *Performance Benchmarking*

In addition, the performance of the proposed DM NT-TFET is benchmarked against the recently proposed TFET (homojunction/heterojunction with device modifications such as complementary doped pockets, hetero-gate dielectric, etc.) based DM biosensors in table I and II. It is evident from tables I and II that the proposed DM NT-TFET provides a significantly better threshold voltage sensitivity (S_{Vth}) and a comparable ON-state current sensitivity ($S_{I_{ON}}$) without introducing significant fabrication complexity as compared to the previously reported TFET-based DM biosensors.

Furthermore, the commercial TCAD simulators do not have a well-defined experimentally calibrated model for emulating noise or diffusion-dominant motion of biomolecules through the nanocavity which limits their capability to perform an accurate analysis of the signal-to-noise ratio (SNR) and the response time of the FET-based biosensors considering the diffusion of biomolecules through the nanocavity. Therefore, we have not performed the analysis of SNR or response time of the biosensors in this work. However, we believe that the thermal noise floor should not affect the detection sensitivity significantly since the ratio of the ON-currents in the presence of biomolecules to the ON-current with air-filled nanocavity is considerably large as shown in Fig. 7.

TABLE II
PERFORMANCE ANALYSIS OF PUBLISHED FET BASED BIOSENSORS CONSIDERING V_{TH} SENSITIVITY

Sl. No.	TFET Based Biosensors	Threshold voltage Sensitivity (S_{Vth})
1	Hetero Gate DM-TFET (L_{gap} = 10 nm, L_{ch} = 50 nm, κ = 10) [14]	0.25
2	Single Pocket DM HTFET (L_{ch} = 42 nm, L_{gap} = 20nm, κ =2.1) [10]	0.14
3	Lateral DM HTFET (L_{ch} = 42 nm, L_{gap} = 10nm, κ = 2) [10]	0.1
4	DM NT-TFET (L_{gap} = 50 nm, L_{ch} = 50 nm, κ = 10) (This work)	0.44

L_{gap}: length of nanocavity, L_{ch}: channel length, κ: dielectric constant of detected biomolecule

V. CONCLUSION

In this work, we have proposed a scalable and extremely energy-efficient NT-TFET biosensor with high sensitivity and selectivity based on the principle of dielectric modulation for efficient detection of label-free bio-analytes. We have performed an extensive investigation of the performance of the proposed DM NT-TFET in the presence of different representative target biomolecules with a dielectric constant (κ) between 2 to 10 and ionized charge densities in the range of -10^{12} C/cm^2 to 10^{12} C/cm^2. Our results indicate that the proposed DM NT-TFET exhibits an extremely high ON-state current sensitivity ($S_{I_{ON}} = 8 \times 10^5$) and threshold voltage sensitivity ($S_{Vth} = 0.44$) for neutral biomolecules, and a high relative change of ~400% in S_{Vth} between keratin-filled nanocavity (κ = 10) and streptavidin-filled nanocavity (κ = 2.1). Furthermore, the sensitivity of the proposed DM NT-TFET biosensor could

be further improved by utilizing different source materials with smaller bandgap such as Ge and InAs or by probing the transient response of the drain current and exploiting the difference in the settling times of the biomolecules. Therefore, the proposed DM NT-TFET is a lucrative alternative to the conventional MOSFET or TFET based biosensors.

REFERENCES

[1] P. Bergveld, "The development and application of FET-based biosensors," *Biosensors*, vol. 2, no. 1, pp. 15–33, 1986. doi: 10.1016/0265-928X(86)85010-6.

[2] H. Im, X.-J. Huang, B. Gu, and Y.-K. Choi, "A dielectric-modulated field effect transistor for biosensing," *Nat. Nanotechnology*, vol. 2, no. 7, pp. 430–434, Jul. 2007. doi: 10.1038/nnano.2007.180.

[3] S. Kalra, M. J. Kumar, and A. Dhawan, "Dielectric-Modulated Field Effect Transistors for DNA Detection: Impact of DNA Orientation," *IEEE Electron Device Letters*, vol. 37, no. 11, pp. 1485-1488, Nov. 2016. doi: 10.1109/LED.2016.2613110.

[4] N. Kannan, S. Kalra, and M. J. Kumar, "Thin Capacitively-Coupled Thyristor as an Ultrasensitive Label-Free Nanogap Biosensor: Proposal and Investigation," *IEEE Sensors Letters*, vol. 1, no. 6, pp. 1-4, Dec. 2017. doi: 10.1109/LSENS.2017.2773147.

[5] J. Choi, J. Han, S. Choi, and Y. Choi, "Analytical Modeling of a Nanogap-Embedded FET for Application as a Biosensor," *IEEE Trans. Electron Devices*, vol. 57, no. 12, pp. 3477-3484, Dec. 2010. doi: 10.1109/TED.2010.2076152.

[6] N. Kannan and M. J. Kumar, "Dielectric-Modulated Impact-Ionization MOS Transistor as a Label-Free Biosensor," *IEEE Electron Device Letters*, vol. 34, no. 12, pp. 1575-1577, Dec. 2013. doi: 10.1109/LED.2013.2283858.

[7] S. Kanungo, S. Chattopadhyay, P. S. Gupta, and H. Rahaman, "Comparative performance analysis of the dielectrically modulated full-gate and short-gate tunnel FET-based biosensors," *IEEE Trans. Electron Devices*, vol. 62, no. 3, pp. 994–1001, Mar. 2015. doi: 10.1109/TED.2015.2390774.

[8] R. Narang, M. Saxena, and M. Gupta, "Comparative Analysis of Dielectric-Modulated FET and TFET-Based Biosensor," *IEEE Trans. Nanotechnol.*, vol. 14, no. 3, pp. 427-435, May 2015. doi: 10.1109/TNANO.2015.2396899.

[9] A. Bhattacharyya, M. Chanda, and D. De, "Performance Assessment of New Dual-Pocket Vertical Heterostructure Tunnel FET-Based Biosensor Considering Steric Hindrance Issue," *IEEE Trans. Electron Devices*, vol. 66, no. 9, pp. 3988-3993, Sept. 2019. doi: 10.1109/TED.2019.2928850.

[10] M. Verma, S. Tirkey, S. Yadav, D. Sharma, and D. S. Yadav, "Performance Assessment of A Novel Vertical Dielectrically Modulated TFET-Based Biosensor," *IEEE Trans. Electron Devices*, vol. 64, no. 9, pp. 3841-3848, Sept. 2017. doi: 10.1109/TED.2017.2732820.

[11] A. Anam, S. Anand, and S. I. Amin, "Design and Performance Analysis of Tunnel Field Effect Transistor with Buried Strained Si1− xGex Source Structure Based Biosensor for Sensitivity Enhancement," *IEEE Sensors Journal*, vol. 20, no. 22, pp. 13178-85, Jun 2020. doi:10.1109/JSEN.2020.3004050

[12] S. Kanungo, S. Chattopadhyay, P. S. Gupta, K. Sinha, and H. Rahaman, "Study and Analysis of the Effects of SiGe Source and Pocket-Doped Channel on Sensing Performance of Dielectrically Modulated Tunnel FET-Based Biosensors, "*IEEE Trans. Electron Devices*, vol. 63, no. 6, pp. 2589-2596, June 2016. doi: 10.1109/TED.2016.2556081.

[13] V. D. Wangkheirakpam, B. Bhowmick, and P. D. Pukhrambam, "N+ Pocket Doped Vertical TFET Based Dielectric-Modulated Biosensor Considering Non-Ideal Hybridization Issue: A Simulation Study," *IEEE Trans. Nanotechnol.*, vol. 19, pp. 156-162, 2020.doi: 10.1109/TNANO.2020.2969206.

[14] S. Ghosh, A. Chattopadhyay, and S. Tewari, "Optimization of Hetero-Gate-Dielectric Tunnel FET for Label-Free Detection and Identification of Biomolecules," *IEEE Trans. Electron Devices*, vol. 67, no. 5, pp. 2157-2164, May 2020. doi: 10.1109/TED.2020.2978499.

[15] D. Sarkar and K. Banerjee, "Proposal for tunnel-field-effect-transistor as ultra-sensitive and label-free biosensors," *Appl. Phys. Lett.*, vol. 100, no. 14, 2012, Art. no. 143108. doi: 10.1063/1.3698093.

[16] A. Gao, N. Lu and Y. Wang, "Robust ultrasensitive tunneling-FET biosensor for point-of-care diagnostics," *Sci. Rep.*, vol. 6, p. 22554, 2016. doi: doi: 10.1038/srep22554

[17] H. M. Fahad and M. M. Hussain, "High-Performance Silicon Nanotube Tunneling FET for Ultralow-Power Logic Applications," *IEEE Trans. Electron Devices*, vol. 60, no. 3, pp. 1034-1039, March 2013. doi: 10.1109/TED.2013.2243151.

[18] A. N. Hanna and M. M. Hussain, "Si/Ge hetero-structure nanotube tunnel field effect transistor," *J. Appl. Phys.*, vol. 117, no. 1, Art. no. 014310, 2015. doi: 10.1063/1.4905423.

[19] A. N. Hanna, H. M. Fahad, and M. M. Hussain, "InAs/Si hetero-junction nanotube tunnel transistors," *Sci. Rep.*, vol. 5, no. 1, p. 9843, 2015. doi: 10.1038/srep09843.

[20] D. Chidambarrao, T. H. Hung, J. W. Sleight, and D. G. Tekleab, "Silicon nanotube MOSFET," U.S. Patent 2012 118 568 A3, Nov. 8, 2012.

[21] G. Musalgaonkar, S. Sahay, R. S. Saxena, and M. J. Kumar, "A Line Tunneling Field-Effect Transistor Based on Misaligned Core–Shell Gate Architecture in Emerging Nanotube FETs," *IEEE Trans. Electron Devices*, vol. 66, no. 6, pp. 2809-2816, June 2019. doi: 10.1109/TED.2019.2910156.

[22] S. Sahay and M. J. Kumar, "Nanotube Junctionless FET: Proposal, Design, and Investigation," *IEEE Trans. on Electron Devices*, vol. 64, no. 4, pp. 1851-1856, April 2017. doi: 10.1109/TED.2017.2672203.

[23] G. Musalgaonkar, S. Sahay, R. S. Saxena, and M. J. Kumar, "Nanotube Tunneling FET With a Core Source for Ultrasteep Subthreshold Swing: A Simulation Study," *IEEE Trans. on Electron Devices*, vol. 66, no. 10, pp. 4425-4432, Oct. 2019. doi: 10.1109/TED.2019.2933756.

[24] S. Sahay and M. J. Kumar, "Junctionless Field-Effect Transistors: Design, Modeling, and Simulation," Hoboken, NJ: Wiley-IEEE Press, 2019.

[25] N. Kumar, S. I. Amin, and S. Anand, "Design and Performance Optimization of Novel Core–Shell Dopingless GAA-Nanotube TFET With Si0.5Ge0.5-Based Source," *IEEE Trans. Electron Devices*, vol. 67, no. 3, pp. 789-795, Jan 2020. doi: 10.1109/TED.2020.2965244

[26] S. Shreya, A. H. Khan, N. Kumar, S. I. Amin, and S. Anand, "Core-Shell Junctionless Nanotube Tunnel Field Effect Transistor: Design and Sensitivity Analysis for Biosensing Application," *IEEE Sensors Journal*, vol. 20, no. 2, pp. 672-679, Oct 2020. doi: 10.1109/JSEN.2019.2944885.

[27] S. Sahay and M. J. Kumar, "Comprehensive analysis of gate-induced drain leakage in emerging FET architectures: Nanotube FETs versus nanowire FETs," *IEEE Access*, vol. 5, pp. 18918–18926, 2017. doi: 10. 1109/access.2017.2751518.

[28] A. Gedam, B. Acharya, and G. P. Mishra, "Design and Performance Assessment of Dielectrically Modulated Nanotube TFET Biosensor," *IEEE Sensors Journal*, vol. 21, no. 15, pp. 16761-16769, 1 Aug.1, 2021. doi: 10.1109/JSEN.2021.3080922.

[29] S. Shreya, A. H. Khan, N. Kumar, S. I. Amin, and S. Anand, "Core-Shell Junctionless Nanotube Tunnel Field Effect Transistor: Design and Sensitivity Analysis for Biosensing Application," *IEEE Sensors Journal*, vol. 20, no. 2, pp. 672-679, 15 Jan.15, 2020. doi: 10.1109/JSEN.2019.2944885.

[30] A.K. Gupta and A. Raman, "Design, Investigation, and Sensitivity Analysis of a Biosensor Based on an Optimized Electrostatically Doped Nanotube TFET," *Journal of Elec. Materi.*, vol. 50, pp. 5462–5471, 2021. doi: 10.1007/s11664-021-09072-7.

[31] S. S. Amiri, A. Gholizadeh, S. Rajabali, Z. Sanaee, and S. Mohajerzadeh, "Formation of Si nanorods and hollow nanostructures using high precision plasma-treated nanosphere lithography," *RSC Adv.*, vol. 4, pp. 12701–12709, Feb. 2014. doi: 10.1039/C4RA00796D

[32] M. S. Parihar and A. Kranti, "Enhanced sensitivity of double gate junctionless transistor architecture for biosensing applications," *Nanotechnology*, vol. 26, no. 14, p. 145201, 2015. doi: 10.1088/0957-4484/26/14/145201.

[33] Dong-Yoon Jang, Young-Pil Kim, Hak-Sung Kim, Sang-Hee Ko Park, Sung-Yool Choi, and Yang-Kyu Choi, "Sublithographic vertical gold nanogap for label-free electrical detection of protein-ligand binding," *Journal of Vacuum Science & Technology B: Microelectronics and Nanometer Structures Processing, Measurement, and Phenomena*, vol. 25, pp. 443-447, 2007. doi: 10.1116/1.2713403

[34] ATLAS Device Simulation Software, Silvaco Int., Santa Clara, CA, USA, 2014.

[35] S. Kanungo, S. Chattopadhyay, K. Sinha, P. S. Gupta, and H. Rahaman, "A Device Simulation-Based Investigation on Dielectrically Modulated Fringing Field-Effect Transistor for Biosensing Applications," *IEEE Sensors Journal*, vol. 17, no. 5, pp. 1399-1406, March, 2017. doi: 10.1109/JSEN.2016.2633621.

[36] J.-H. Ahn, J.-Y. Kim, M. Im, J.-W. Han, and Y.-K. Choi, "A nanogap-embedded nanowire field effect transistor for sensing applications: Immunosensor and humidity sensor*," in Proc. 14th Int. Conf. Miniaturized Syst. Chem. Life Sci.*, Groningen, The Netherlands, Oct. 2010, pp. 1301–1303.

[37] C. Kim, J. Ahn, K. Lee, C. Jung, H. G. Park, and Y. Choi, "A New Sensing Metric to Reduce Data Fluctuations in a Nanogap-Embedded Field-Effect Transistor Biosensor," *IEEE Trans. Electron Devices*, vol. 59, no. 10, pp. 2825-2831, Oct. 2012. doi: 10.1109/TED.2012.2209650.

[38] S. Mukhopadhyay, D. Sen, B. Goswami, and S. K. Sarkar, "Performance Evaluation of Dielectrically Modulated Extended Gate Single cavity InGaAs/Si HTFET based Label-free Biosensor Considering Non-ideal Issues," *IEEE Sensors Journal*, vol. 21, no. 4, pp. 4739-4746, 15 Feb.15, 2021. doi: 10.1109/JSEN.2020.3033576.

[39] R. Gautam, M. Saxena, R. S. Gupta, and M. Gupta, "Numerical model of gate-all-around MOSFET with vacuum gate dielectric for biomolecule detection," *IEEE Electron Device Lett.*, vol. 33, no. 12, pp. 1756–1758, Dec. 2012. doi: 10.1109/LED.2012.2216247.

[40] S. Sahay and M. J. Kumar, "Controlling the Drain Side Tunneling Width to Reduce Ambipolar Current in Tunnel FETs Using Heterodielectric BOX," *IEEE Trans. Electron Devices*, vol. 62, no. 11, pp. 3882-3886, Nov. 2015. doi: 10.1109/TED.2015.2478955.

[41] P. Dwivedi, R. Singh, B. S. Sengar, A. Kumar, and V. Garg, "A New Simulation Approach of Transient Response to Enhance the Selectivity and Sensitivity in Tunneling Field Effect Transistor-Based Biosensor," *IEEE Sensors Journal*, vol. 21, no. 3, pp. 3201-3209, 1 Feb.1, 2021. doi: 10.1109/JSEN.2020.3028153.

[42] Sungho Kim, Jee-Yeon Kim, Jae-Hyuk Ahn, Tae Jung Park, Sang Yup Lee, and Yang-Kyu Choi, "A charge pumping technique to identify biomolecular charge polarity using a nanogap embedded biotransistor", *Appl. Phys. Lett.*, vol. 97, p. 073702, 2010. doi: 10.1063/1.3473819

[43] A. Bhattacharyya, M. Chanda and D. De, "Analysis of Partial Hybridization and Probe Positioning on Sensitivity of a Dielectric Modulated Junctionless Label Free Biosensor," *IEEE Trans. Nanotechnol.*, vol. 19, pp. 719-727, 2020. doi: 10.1109/TNANO.2020.3025544.

[44] S. J. Mukhopadhyay, B. Majumdar, K. N. Chappanda, S. C. Mukhopadhyay and S. Kanungo, "Performance Analysis of the Diagonal Tunneling-Based Dielectrically Modulated Tunnel FET for Bio-Sensing Applications," *IEEE Sensors Journal*, vol. 21, no. 19, pp. 21643-21652, Oct. 2021. doi: 10.1109/JSEN.2021.3103998.

[45] S. Kumar, Y. Singh, B. Singh and P. K. Tiwari, "Simulation Study of Dielectric Modulated Dual Channel Trench Gate TFET-Based Biosensor," *IEEE Sensors Journal*, vol. 20, no. 21, pp. 12565-12573, Nov. 2020. doi: 10.1109/JSEN.2020.3001300.